

Received 19 February 2024, accepted 7 March 2024, date of publication 11 March 2024, date of current version 18 March 2024.

Digital Object Identifier 10.1109/ACCESS.2024.3375887

## RESEARCH ARTICLE

# Design, Modeling, and Simulation of a Novel Electromagnetic Linear Actuator for Linear Motion

SHUAIBY MOHAMED<sup>1,2</sup>, (Member, IEEE), YOUNGWOON IM<sup>2</sup>, HYEONSANG SHIN<sup>2</sup>,  
YOUNGSHIK KIM<sup>2</sup>, AND BUHYUN SHIN<sup>2</sup>

<sup>1</sup>Department of Mechatronics Engineering, Faculty of Engineering, Assiut University, Assiut 71516, Egypt

<sup>2</sup>Department of Mechanical Engineering, Hanbat National University, Deajeon 34158, South Korea

Corresponding author: Buhyun Shin (jedidiah@hanbat.ac.kr)

This work was supported by the Basic Science Research Program through the National Research Foundation of Korea (NRF) funded by the Ministry of Education under Grant (No. NRF-2020R111A3070333).

**ABSTRACT** This paper presents the design, modeling, and simulation of a compact Electromagnetic Linear Actuator (ELA) and its application to a linear motion mechanism. The proposed actuator consists of a coil and a permanent magnet and can generate a linear motion when an alternating current is applied to the coil. Its overall dimensions are 20 mm (W) × 15 mm (H) × 15 mm (D) while the weight is 7 g. The proposed actuator can be controlled in terms of position using an open-loop system. A mathematical model is created for the proposed actuator, and theoretical analysis is performed to examine the actuator dynamic model. The simulation results are validated experimentally by manufacturing a physical prototype. Therefore, the proposed actuator generates an electromagnetic force of 0.1 N at 10 V (0.07 A), then our actuator able to achieve a displacement of 0.2 mm. Moreover, the experimental resonance frequency is measured at 70 Hz and the bandwidth of 80 Hz. Finally, the overall system performance is evaluated by integrating the developed actuator into the linear motion mechanism. We investigate the stick-slip motion of the linear mechanism without feedback control, dedicating sufficient time to both the slip phase and the stick phase. The experimental results show that the linear motion mechanism travels with speed 6 mm s<sup>-1</sup> with a frequency of 30 Hz.

**INDEX TERMS** Electromagnetic actuator, linear motion, stick-slip, linear actuator.

## I. INTRODUCTION

Nowadays, various types of actuators have been employed in the development of micro robots for medical or industrial applications. However, small-sized actuators often lack the necessary power compared to biological living systems, posing a challenge for robot applications [1], [2], [3], [4], [5]. To overcome this limitation, researchers have explored the use of smart materials to enhance the functionalities and capabilities of miniaturized robots. However, the development of a fully autonomous and practically relevant miniaturized robot system remains an ongoing endeavor. While advancements have been made in micro

robot development, achieving sufficient power and complete autonomy for practical applications continues to present challenges. One specific area of research involves the use of electromagnetic oscillatory actuators in micro mobile robots. These actuators possess a simple structure consisting of cores, coils, magnets, and yokes. They are capable of generating oscillatory motion and have been employed in various types of micro robots, including tadpole robots, 2-legged robots, and 4-legged robots [6]. A miniaturized dual electromagnetic oscillatory actuator has been proposed, which includes two magnets, a coil, and a yoke [7]. In that system the dynamic characteristics, torque, and restoring constants of these actuators have been determined using finite element simulation techniques. The utilization of electromagnetic actuators in micro robots offers advantages such as

The associate editor coordinating the review of this manuscript and approving it for publication was Giovanni Angiulli<sup>1</sup>.

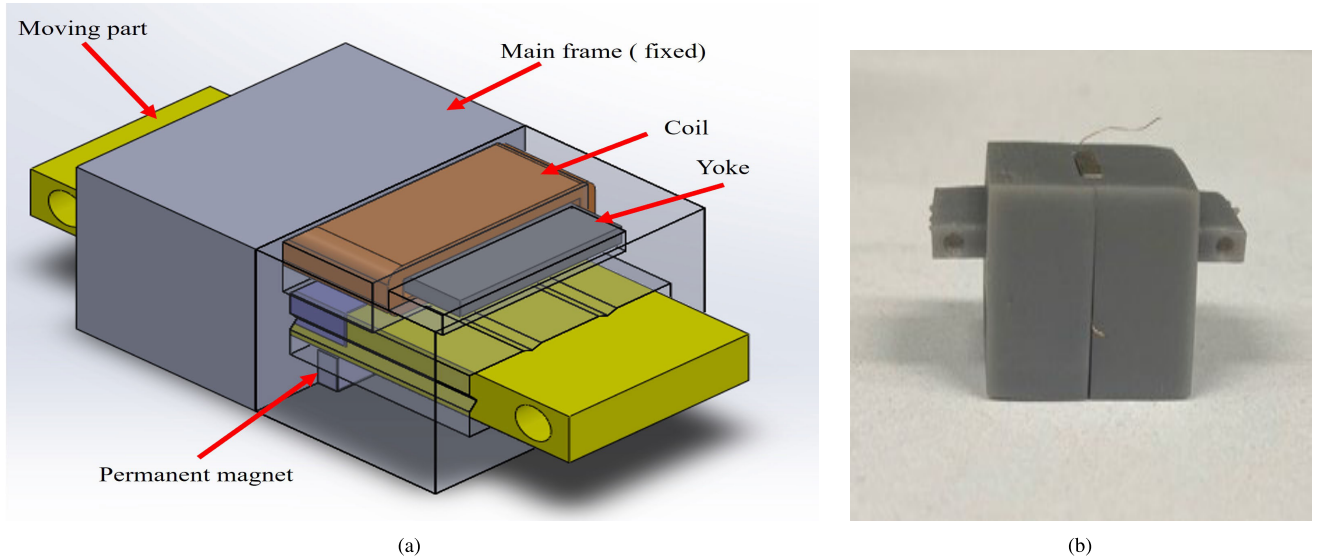


FIGURE 1. (a) 3D model of the proposed electromagnetic linear actuator (b) Physical prototype.

generating large forces, providing substantial displacement, and consuming less power [8]. These actuators have been specifically customized and developed for micro robots, addressing the limitations of conventional electromagnetic actuators [9].

A compact electromagnetic oscillatory actuator has been proposed for micro robots, including tadpole, 2-legged, and 4-legged robots [10]. A miniaturized tadpole-like robot using an electromagnetic oscillatory actuator has been developed, enabling undulatory propulsion and directional control. Overall, while there have been advancements in micro robot development, there are still challenges in achieving sufficient power and fully autonomous systems for practical applications.

The movement of micro robots has been made possible through the utilization of various miniature actuators, including piezoelectric (PZT), shape memory alloy (SMA), polymer, and electromagnetic actuators. Piezoelectric actuators offer several advantages for micro robots, including fast response, size reduction, and high output power [11], [12], [13], [14], [15], [16], [17]. However, they do have some drawbacks, such as the requirement of high input voltage and additional structures to amplify small deformations. Shape Memory Alloy (SMA) actuators are known for their simple structure and reasonable power output [18], [19], [20], [21], [22]. However, they do come with certain drawbacks, including limited speed and a delayed response. In recent times, there has been extensive research on soft polymer actuators, with Ionic Polymer Metal Composite (IPMC) emerging as a prominent choice for applications in wormlike, legged, tadpole, and fish robots [23], [24], [25], [26]. IPMC actuators offer several advantages, including significant bending displacement, low input voltage requirements, and underwater mobility. However, they do have limitations, such as relatively weak output power and reduced displacement when operated in air.

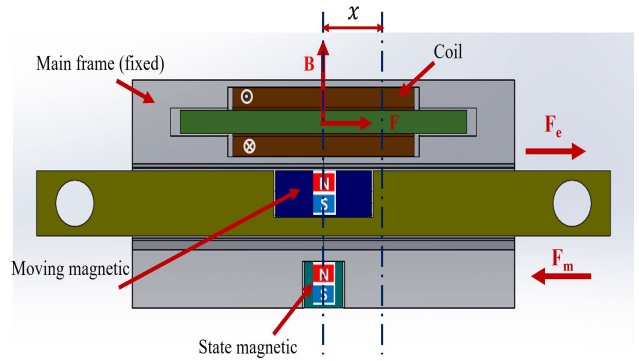


FIGURE 2. Cross section area of ELA: Lorentz force ( $F$ ), a magnetic field ( $B$ ),  $\otimes$  current in,  $\odot$  current out, and Forces  $F_m$ ,  $F_e$ .

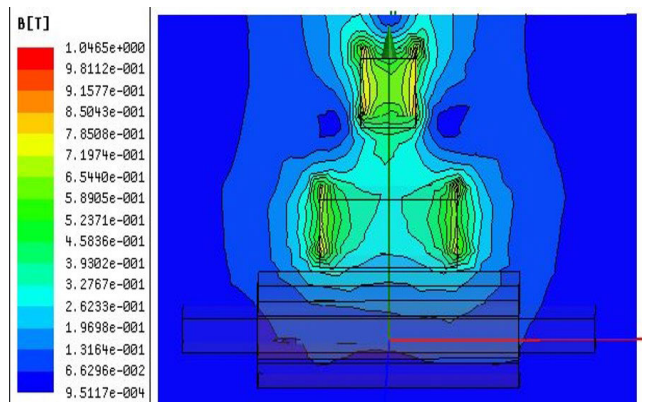


FIGURE 3. Simulation results of magnetic flux density in a proposed electromagnetic linear actuator.

Actuators using electromagnetic technology have gained extensive utilization across diverse engineering applications owing to their precision and dependability. These actuators, encompassing motors, solenoids, and relays, have undergone constant advancements and are now ubiquitous in everyday devices. The progress made in developing high performance

electromagnetic actuators has effectively tackled challenges related to high current, noise, and bulky dimensions, resulting in actuators that boast uncomplicated designs, affordability, consistent performance, and substantial force output. Electromagnetic actuators have several advantages such as rapid response, simple control law, and cost-effectiveness. Most micro robots that require oscillating or reciprocal motions tend to use other types of actuators. Morrey [27] describes the development of novel highly mobile small robots called “Mini-Whigs” that combine the speed and simplicity of wheels with the climbing mobility of legs. In the field of bio-mimic mobile robots and optical devices like LiDAR and barcode mirrors, small actuators are important for compactness and improved performance. The mass and dimensions of these components play a crucial role in achieving agility, maneuverability, and precise mechanical movements. Reducing the size and weight of actuators enables the development of smaller and more efficient low-cost systems.

This study mainly aims to develop an electromagnetic linear actuator with a compact design and its application to a linear motion mechanism. Its overall dimensions are 20 mm (W)  $\times$  15 mm (H)  $\times$  15 mm (D) while the weight is 7 g. A mathematical model is created for the proposed actuator, and theoretical analysis is performed to examine the actuator dynamic model. The simulation results are validated experimentally by manufacturing a physical prototype. Furthermore, a finite element analysis is conducted in simulation and experiments to compute the magnetic flux within the ELA system. Finally, the overall system performance is evaluated by integrating the developed actuator into the linear motion mechanism.

The paper is organized as follows: Section II presents the design, dynamic modeling, and working principle of the electromagnetic linear actuator. Section III describes the linear motion mechanism along with simulation and experimental results. In Section IV, we provide a conclusion and discuss the work.

## II. ELECTROMAGNETIC LINEAR ACTUATOR

### A. LINEAR ACTUATOR DESIGN

Figure 1 shows the novel linear electromagnetic actuator that we have designed and manufactured. This proposed actuator stands out for its compact design, measuring 20 mm  $\times$  15 mm  $\times$  15 mm and weighing 7 g. It incorporates key components including a coil, yoke, moving magnet, fixed magnet, and moving part. The main frame and moving part were produced using SLA-type 3D printer with a minimum layer thickness of 0.1 mm. we used Neodymium (ND35) as the material for all the permanent magnets, as it is currently the strongest commercially available option. To focus and sustain the magnetic field generated by the coils, a soft iron yoke AISI 1020 is affixed inside them. Additionally, the main frame contains an energized coil made up of approximately 1312 turns and has a resistance of 140  $\Omega$ .

TABLE 1. Physical parameters of electromagnetic linear actuator.

Symbol	Parameter		Value	Unit
$m$	Mass of ELA	Measured	7	g
$R$	Resistance	Measured	140	$\Omega$
$K_m$	Reinstating force constant	Measured	484.59	mN/mm
		Simulated	437.27	mN/mm
$K_t$	Force constant	Measured	1.6617	N/A
		Simulated	1.6686	N/A

### B. DYNAMIC MODELLING AND WORKING PRINCIPAL

The oscillatory actuator experiences two types of forces. The magnetic force between the magnet and the steel core, known as the reinstating force, holds the movers in the central position. The fundamental concept that governs the operation of the proposed ELA revolves around the generation of Lorentz force ( $F$ ) by employing current-carrying coils in conjunction with permanent magnets. The proposed actuator is driven by the Lorentz force ( $F$ ), which is generated when a current ( $I$ ) flows through a coil located within a magnetic field ( $B$ ) as shown in Figure 2. According to Fleming’s left-hand rule, when a current passes through a coil placed in a magnetic field, it results in an electromagnetic force  $F_e$  of moving magnet directed to the right. As a result, the actuator moves in the same direction to the right, as it is attached to a moving magnet. When the moving magnet creates a displacement to the right side, a magnetic force  $F_m$  occurs between the moving magnet and the fixed magnet due to the attraction force between opposite poles. The different poles of the magnets result in an attraction force that acts towards the left side. The moving frame with the moving magnet comes to a stop at the right-side displacement when the electromagnetic force  $F_e$  generated by the current-carrying coil is equal to the magnetic force  $F_m$  between the moving magnet and the fixed magnet. At this point, the forces acting on the system are balanced, resulting in the cessation of further displacement. Decreasing the current ( $I$ ) reduces the electromagnetic force  $F_e$  and allows the magnetic force  $F_m$  between the magnets to bring the moving magnet back to its initial position. When the current reaches zero, the moving magnet returns to its center position, so open-loop control is possible.

The actuator system is theoretically based on a DC motor, making its dynamic model similar to that of a DC motor. The equation for the dynamic model can be written as

$$m\ddot{x} + F_m = F_e \quad (1)$$

$$F_m = K_m x \quad (2)$$

$$F_e = K_t I \quad (3)$$

$$V = K_e \dot{x} + IR \quad (4)$$

where  $m, \ddot{x}, \dot{x}, x$  are the mass of electromagnetic linear actuator, linear acceleration, linear velocity, and displacement, respectively.  $F_m, F_e$  are the magnetic force, and electromagnetic force, respectively, and they are assumed to

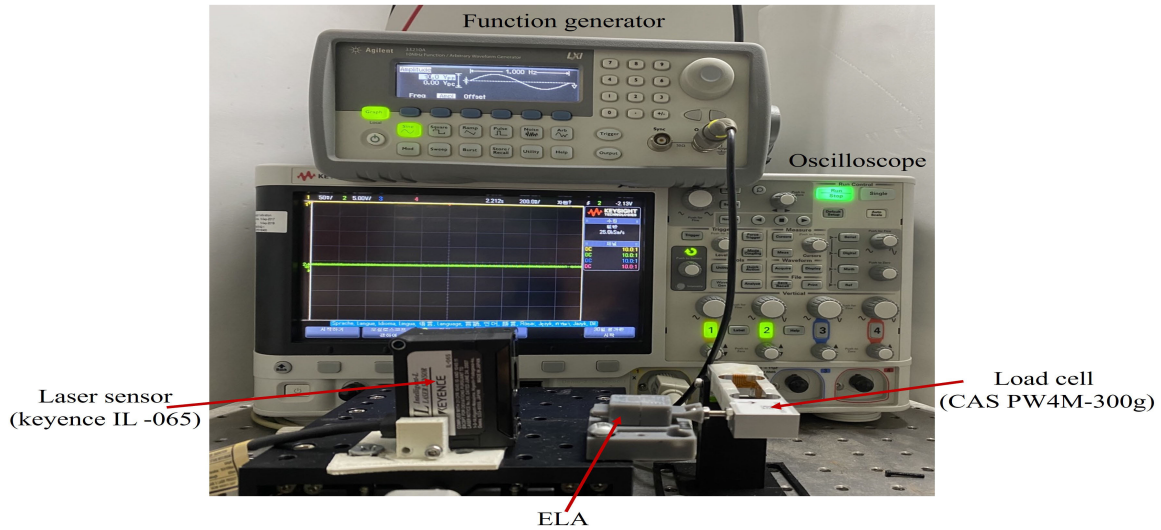


FIGURE 4. Overview of the experimental system.

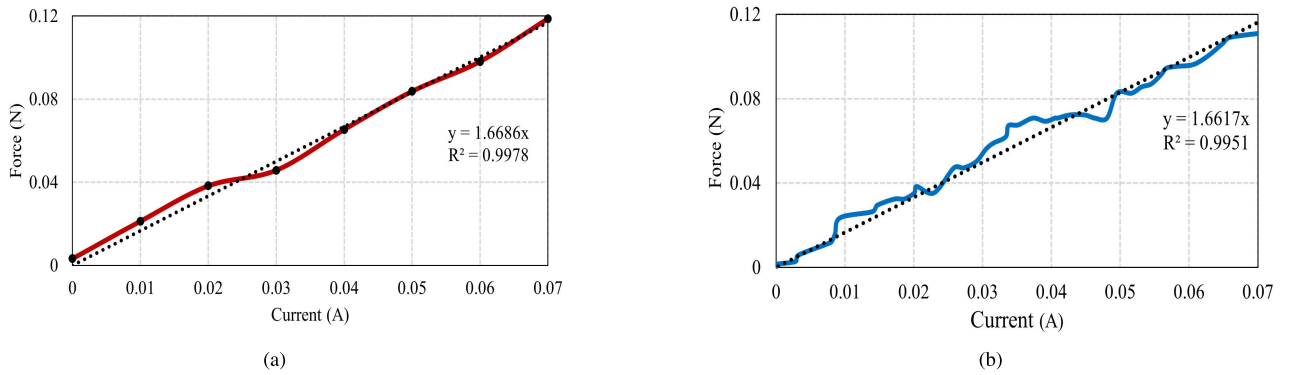


FIGURE 5. Force generated with respect to the applied current of the electromagnetic linear actuator (a) Simulation results and (b) Experimental results.

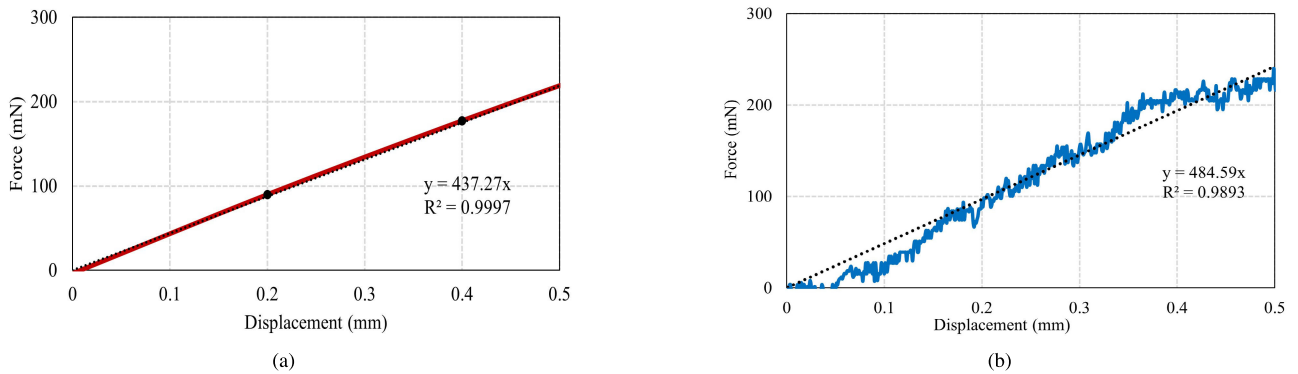


FIGURE 6. Force generated with respect to the displacement of the electromagnetic linear actuator (a) Simulation results and (b) Experimental results.

have a linear relationship.  $K_m$ ,  $K_t$ ,  $K_e$  are the reinstating force constant, force constant, and back-emf constant, respectively. We made the assumption that the force constant and the back-emf constant are frequently the same as in a DC motor.  $V$ ,  $I$ ,  $R$  are the applied voltage, current, and resistance of the coil respectively. The electrical circuit's indication component was ignored. We assumed there is no friction between the main frame and the moving magnetic (moving part), therefore there isn't no transition from static to dynamic friction.

The relationship between the input and the output is as follows.

$$\frac{X}{V} = \frac{K_t/R}{mS^2 + (K_tK_e/R)S + K_m} \quad (5)$$

where  $V$  represents the input as the applied voltage and  $X$  represents the output as the linear displacement.

In order to validate the performance of the developed actuator, simulations and experimental analyses were conducted by using a finite element analysis (FEA). It is necessary to

measure the physical parameters, such as mass and resistance. Additionally, the reinstating constant and the electromagnetic linear actuator constant are determined by utilizing both finite element simulation and measurement data. Figure 3 presents the simulation results of the magnetic flux density obtained through the FEA. We conducted the magnetic field analysis to evaluate the effectiveness of the magnetic field between the moving magnet and the fixed magnet, as well as between the moving magnet and the core. The objective was to determine if the magnetic field strength was suitable for the intended purpose. Instead of focusing on achieving the highest magnetic flux density, which could lead to challenges like heat generation and excessive force requirement, the analysis aimed to identify the minimum force necessary to achieve the desired displacement. By doing so, the analysis aimed to find the optimal balance between magnetic field strength and the required force for successful operation.

### C. SIMULATION AND EXPERIMENTAL RESULTS

In order to evaluate the dynamic performances of the developed actuator, a physical prototype of our electromagnetic linear actuator was manufactured as shown in Figure 1 (b). An overview of the electromagnetic linear actuator experimental system is provided in Figure 4. A laser displacement sensor (Keyence IL-065), used for measuring the horizontal displacement of the proposed actuator. A load cell (CAS PW4M-300g) used for measuring the magnetic force. In addition, the electrical current needed to activate the coils was provided by a function generator. A hardware setup was created using a power Op-Amp L272 for the construction of a simple voltage follower circuit. To obtain the reinstating force constant  $K_m$  and the force constant  $K_f$  we conducted measurements using a load cell to determine the forces.

The measurements were taken as a function of the input current and displacement. We then compared these measurements with the results obtained from the FEA simulation, which are depicted in figures 5 and 6, respectively. The results obtained from the simulations and experiments demonstrate the relationship between the applied current and the resulting force produced by an electromagnetic linear actuator are shown in figure 5. The reinstating constant  $K_m$  is calculated using Equation 2 from simulating and measuring the magnetic force at each actuator displacement. From the experimental data, the value of  $K_m$  is found to be 484.59 mN/mm, while the simulation yields a value of 437.27 mN/mm for  $K_m$ . The results obtained from the simulations and experiments demonstrate the relationship between the displacement and the resulting force produced by an electromagnetic linear actuator are shown in Figure 6.

Similarly the force constant  $K_f$  is calculated using Equation 3 from simulating and measuring the magnetic force at each actuator input current. From the experimental data, the value of  $K_f$  is found to be 1.6617 N/A, while the simulation yields a value of 1.6686 N/A for  $K_f$ . In fact, the observed disparities between the simulation and actual results can be explained by the existence of mechanical

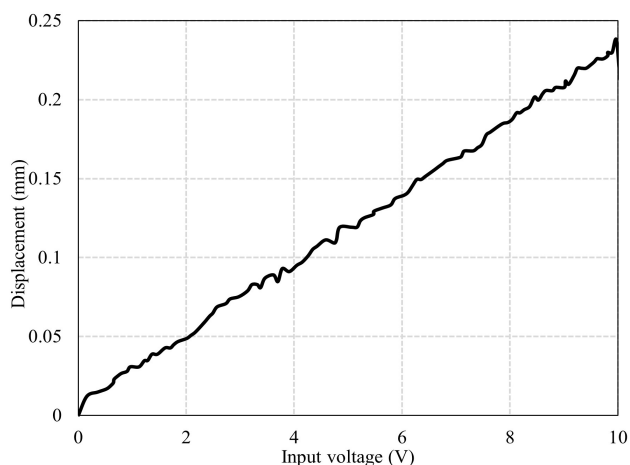


FIGURE 7. Displacement of the electromagnetic linear actuator due to voltages.

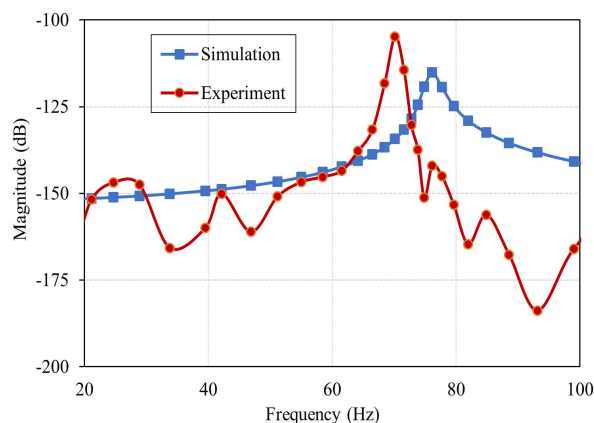


FIGURE 8. Frequency response of the electromagnetic linear actuator.

errors, variations in material properties, and differences in simulation settings. Nevertheless, the data acquired clearly shows that our electromagnetic linear actuator (ELA) exhibits a linear behavior in spite of these factors. Therefore, all the results have been successfully linearized, and the correlation coefficients are all above 99%, demonstrating a robust linear relationship between the variables. We summarized the physical parameters of the electromagnetic linear actuator, including both the simulation and experimental data, in Table 1.

In addition, we conducted an experiment to evaluate open-loop control and dynamics of the ELA system. Figure 7 illustrates the experimental result of the electromagnetic linear actuator employing open-loop control, where the motion of the moving frame ceases at the equilibrium position when the forces  $F_e$  and  $F_m$  become equal. We create the sinusoidal input from 1 Hz to 100 Hz using the function generator. The oscilloscope stores the displacement signals of the ELA that were determined by the laser displacement sensor. Figure 8 presents the results of the experimental dynamic response analysis, after the analysis using the Fast Fourier Transform (FFT), and it is compared to the theoretical frequency responses based on Equation 5. Two scenarios are

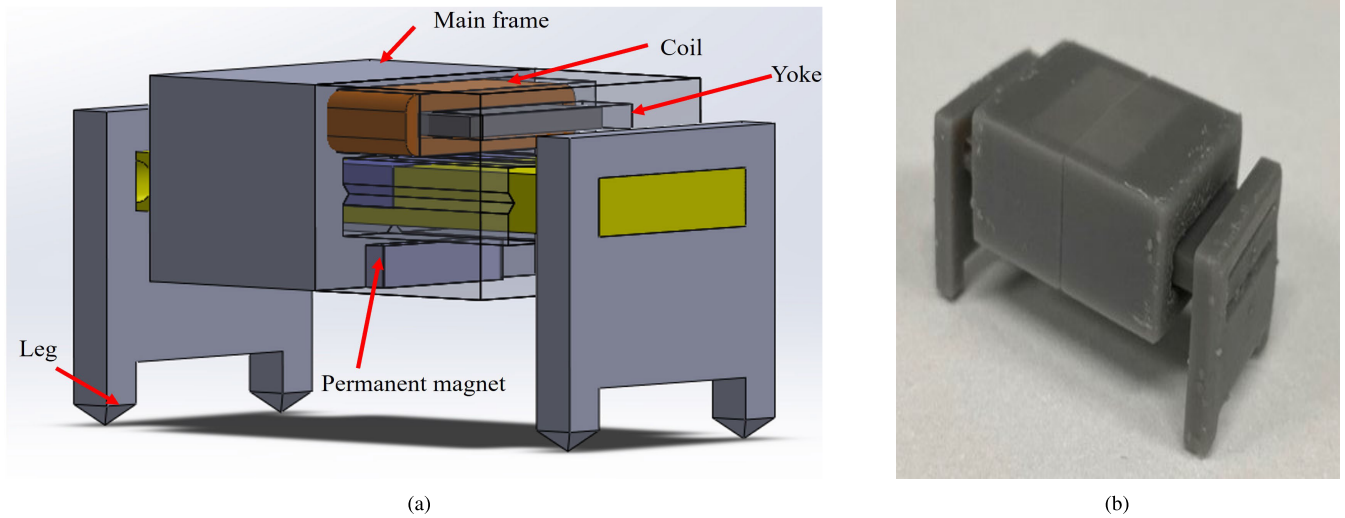


FIGURE 9. (a) 3D model of the linear mechanism using electromagnetic linear actuator (b) Physical prototype.

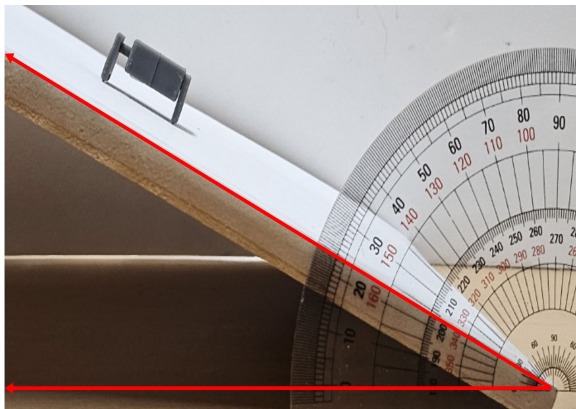


FIGURE 10. Static friction coefficient measurement.

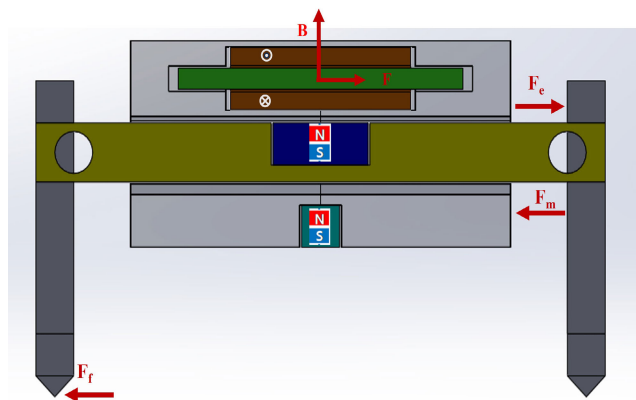


FIGURE 11. Schematic diagram of the linear mechanism using linear actuator: Lorentz force ( $F$ ) is generated when a magnetic field ( $B$ ).

considered, utilizing simulation and experimental data for the force and restoring constants ( $K_m$  and  $K_f$ ). The peak values in Figure 8 indicate an input voltage of  $\pm 5$  V (30 mA) for the experimental ELA. The experimental and theoretical resonance frequencies are measured to be 70 Hz and 76 Hz, respectively. The experiment indicates a bandwidth of 80 Hz.

Based on the experimental findings, the electromagnetic linear actuator is well-suited for a linear mechanism. These linear mechanism can utilize the actuator’s resonance to enhance their movement speed effectively.

### III. LINEAR MOTION MECHANISM

#### A. LINEAR MOTION MECHANISM DESIGN

We developed a linear mechanism that effectively utilizes the specially designed actuator to enable both forward and backward movement. The linear mechanism incorporates a leg attachment connected to the actuator’s mover, as clearly illustrated in Figure 9.a. With dimensions measuring 20 mm  $\times$  15 mm  $\times$  30 mm (length  $\times$  width  $\times$  height), the linear mechanism design includes the integration of the leg length directly into the actuator. The total weight of the linear mechanism amounts to 8 g, with the body weighing 7 g and the legs weighing 1 g. To minimize the friction with the floor, the legs are thoughtfully designed with square pyramid-shaped ends, ensuring point contact. We have successfully created a prototype of the linear mechanism featuring the grafted leg, as depicted in Figure 9.b. Figure 10 shows an experimental approach for determining the static friction coefficient. In the experiment, the robot’s angle of inclination was measured as it was about to slide, which made it possible to calculate the static friction coefficient. The measured angle was approximately 23°, which corresponds to a friction coefficient value of 0.03 on a paper.

#### B. STICK-SLIP MOTION MECHANISM

Figure 11 shows the free body diagram of the linear mechanism, which is considered as a stick-slip mechanism. It illustrates the forces involved in the linear actuator’s generation of linear motion. There are three forces applied in the actuator namely magnetic force, electromagnetic force, and friction force. The equation for the dynamic model of the

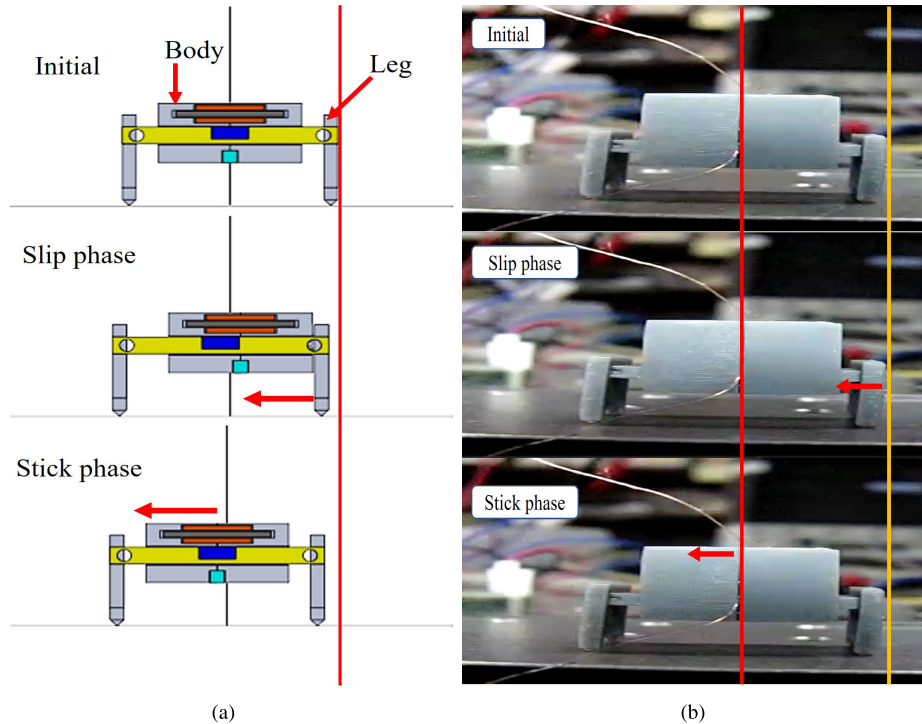


**FIGURE 12.** Schematic diagram of stick-slip mechanism during one step (a) Simulation results and (b) Experimental results.

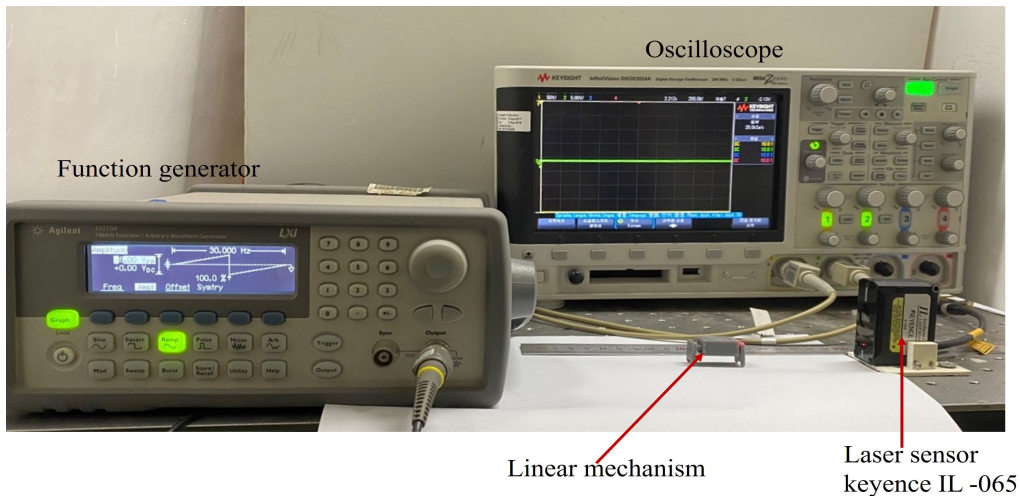


**FIGURE 13.** Overview of the experimental setup for measuring the movement of the linear mechanism.

stick-slip motion mechanism can be written as

$$M\ddot{x} = F_e(x, t) - F_m(x, t) - F_f \quad (6)$$

where  $M, \ddot{x}, \dot{x}, x$  are the mass, linear acceleration, linear velocity, and displacement, respectively.  $F_m, F_e, F_f$  are the magnetic force, electromagnetic force, and friction force respectively. We apply the principle of work and energy as equation 7 to solve the nonlinear differential equation 6.

$$\frac{1}{2}Mv_1^2 - \frac{1}{2}Mv_2^2 = \int_{x_1}^{x_2} (F_e(x, t) - F_m(x, t) - F_f)dx \quad (7)$$

where  $v_1, v_2$  represent the velocities at the positions  $x_1, x_2$  of the linear mechanism, respectively.

The stick-slip movement of the linear mechanism was observed in two phases: We conducted experiments and simulations to verify the stick-slip movement during one step of the linear mechanism, as shown in Figure 12.

- Initial: The linear mechanism remains stationary and the body remains fixed.
- Slip phase: The legs move to the left while the body remains fixed.
- Stick phase: The legs come to a halt due to friction force, and the body moves to the left propelled by the magnetic force.

This confirms that the linear mechanism undergoes movement in these two distinct phases.

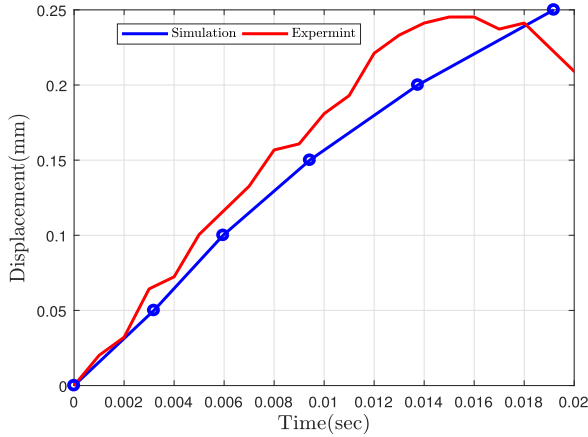


FIGURE 14. One step motion of the stick-slip leg.

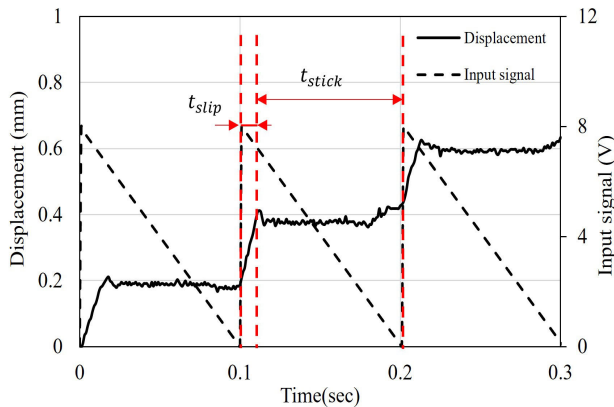


FIGURE 15. Leg displacement at 10 Hz with 8 V saw input.

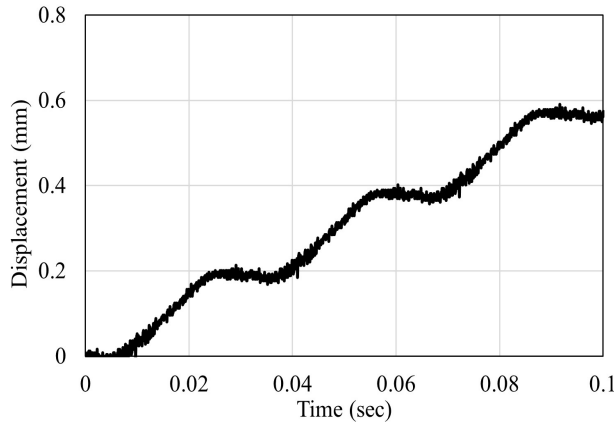


FIGURE 16. Leg displacement at 30 Hz with 8 V saw input.

C. EXPERIMENT OF THE LINEAR MECHANISM

1) EXPERIMENTAL SETUP

An overview of the the experimental setup for measuring the movement of the linear mechanism is shown in Figure 13. The electrical current needed to activate the coils was provided by a function generator. A hardware setup was created using a power Op-Amp L272 for the construction of a simple voltage follower circuit. A laser displacement sensor (Keyence IL-065), used for measuring the horizontal displacement of the linear mechanism.

2) EXPERIMENTAL RESULTS

We conducted an experiment to measure the displacement of the linear mechanism using the proposed electromagnetic linear actuator. Figure 14 shows the one step motion of the stick-slip linear mechanism. Through both simulation and experimentation, the displacement of the linear mechanism for the stick-slip leg’s one-step motion is measured for a range of the input voltage. Furthermore, we conduct an experiment to measure the displacement of the leg using a saw input voltage of 8 V, ranging in frequency from 10 Hz to 30 Hz. At a frequency of 10 Hz, the time  $t_{slip}$  of the slip phase was 13 ms and the time  $t_{stick}$  of the stick phase was 87 ms. Therefore, the total time for one step was 100 ms shown in Figure 15. As a result, the linear mechanism exhibited a moving speed of 2.2 mm/s. We experimented with several frequencies and found that 30 Hz was the optimal frequency for the linear mechanism. The time  $t_{slip}$  of slip phase was 30 ms and the time  $t_{stick}$  of the stick phase lasted 5 ms at this frequency as shown in Figure 16. As a result, one step took a total of 35 ms to complete. The outcome was that the linear mechanism moved at a speed of 6 mm/s as opposed to the prior speed of 2.2 mm/s. We observed stick-slip motion in the system at 10 Hz, but as the frequency increased to 30 Hz, we noticed a reduction in the time  $t_{stick}$  of the stick phase, resulting in smoother operation.

IV. CONCLUSION

This paper presents the design, modeling, and simulation of an electromagnetic linear actuator with its application to a linear motion mechanism. We conducted modeling of the developed actuator and performed theoretical analysis to examine its dynamic model. A physical prototype of the actuator was constructed, and extensive testing was conducted to validate the simulation results. A finite element analysis was employed to compute the magnetic flux within the ELA system, and experiments were conducted using a physical prototype that had dimensions of 20 mm (W) × 15 mm (H) × 15 mm (D) and weighing 7 g. Performance metrics, including frequency response, power consumption, and efficiency, were measured and assessed. As a result, our actuator generates a force of 0.12 N in simulation and 0.1 N in experimental measurements when supplied with the same current. Moreover, the experimental resonance frequency is measured at 70 Hz, while the theoretical resonance frequency is determined to be 76 Hz. The experiment indicates a bandwidth of 80 Hz. Furthermore, we proceeded with the integration of the developed actuator into the linear motion mechanism and conducted extensive testing to evaluate the overall performance of the system. The experimental results show that the linear motion mechanism travels with speed 6 mm s<sup>-1</sup> with a frequency of 30 Hz. Future work will focus on integrating the proposed linear actuator into micro-robotics for medical and industrial applications.



## REFERENCES

- [1] K. Zhu, H. Li, X. Zhang, T. Xu, and S. Li, "A miniature electromagnetic linear actuator with 3D MEMS coil," *IEEE Electron Device Lett.*, vol. 44, no. 10, pp. 1732–1735, Oct. 2023.
- [2] M. Wang, T. Wu, R. Liu, Z. Zhang, and J. Liu, "Selective and independent control of microrobots in a magnetic field: A review," *Engineering*, vol. 24, pp. 21–38, May 2023.
- [3] Z. Li, C. Li, L. Dong, and J. Zhao, "A review of microrobot's system: Towards system integration for autonomous actuation in vivo," *Micromachines*, vol. 12, no. 10, p. 1249, Oct. 2021.
- [4] V. K. Bandari and O. G. Schmidt, "System-engineered miniaturized robots: From structure to intelligence," *Adv. Intell. Syst.*, vol. 3, no. 10, Oct. 2021, Art. no. 2000284.
- [5] J. K. Schonebaum, F. Alijani, and G. Radaelli, "Review on mobile robots that exploit resonance," *Proc. Inst. Mech. Eng. C, J. Mech. Eng. Sci.*, vol. 235, no. 24, pp. 7907–7924, Dec. 2021, doi: 10.1177/095440622111036923.
- [6] B. H. Shin and S.-Y. Lee, "Micro mobile robots using electromagnetic oscillatory actuator," in *Proc. 4th IEEE RAS EMBS Int. Conf. Biomed. Robot. Biomechatronics (BioRob)*, Jun. 2012, pp. 575–580.
- [7] B. H. Shin, K.-M. Lee, and Y. Kim, "Miniaturized dual electromagnetic oscillatory actuator for legged locomotion of micro mobile robots," *Int. J. Control Autom.*, vol. 7, no. 8, pp. 245–256, Aug. 2014.
- [8] B. Shin, Y. Kim, J. Paik, and K.-M. Lee, "Miniaturized twin-legged robot with an electromagnetic oscillatory actuator," *J. Bionic Eng.*, vol. 15, no. 1, pp. 106–113, Jan. 2018.
- [9] H. Lu, J. Zhu, Z. Lin, and Y. Guo, "An inchworm mobile robot using electromagnetic linear actuator," *Mechatronics*, vol. 19, no. 7, pp. 1116–1125, Oct. 2009.
- [10] B. H. Shin, K.-M. Lee, and S.-Y. Lee, "A miniaturized tadpole robot using an electromagnetic oscillatory actuator," *J. Bionic Eng.*, vol. 12, no. 1, pp. 29–36, Mar. 2015.
- [11] M. Karpelson, G.-Y. Wei, and R. J. Wood, "Driving high voltage piezoelectric actuators in microbotic applications," *Sens. Actuators A, Phys.*, vol. 176, pp. 78–89, Apr. 2012.
- [12] Q. S. Nguyen, S. Heo, H. C. Park, and D. Byun, "Performance evaluation of an improved fish robot actuated by piezoceramic actuators," *Smart Mater. Struct.*, vol. 19, no. 3, Mar. 2010, Art. no. 035030.
- [13] S. Martel, "Fundamental principles and issues of high-speed piezoactuated three-legged motion for miniature robots designed for nanometer-scale operations," *Int. J. Robot. Res.*, vol. 24, no. 7, pp. 575–588, Jul. 2005.
- [14] A. T. Baisch, C. Heimlich, M. Karpelson, and R. J. Wood, "HAMR3: An autonomous 1.7g ambulatory robot," in *Proc. IEEE/RSJ Int. Conf. Intell. Robots Syst.*, Sep. 2011, pp. 5073–5079.
- [15] K. L. Hoffman and R. J. Wood, "Myriapod-like ambulation of a segmented microrobot," *Auto. Robots*, vol. 31, no. 1, pp. 103–114, Jul. 2011.
- [16] Q. S. Nguyen, S. Heo, H. C. Park, N. S. Goo, T. Kang, K. J. Yoon, and S. S. Lee, "A fish robot driven by piezoceramic actuators and a miniaturized power supply," *Int. J. Control, Autom. Syst.*, vol. 7, no. 2, pp. 267–272, Apr. 2009.
- [17] J. Escareno, J. Abadie, E. Piat, and M. Rakotondrabe, "Robust micro-positioning control of a 2DOF piezocantilever based on an extended-state LKF," *Mechatronics*, vol. 58, pp. 82–92, Apr. 2019.
- [18] H. Zhang, B. Xu, Y. Ouyang, Y. Wang, H. Zhu, G. Huang, J. Cui, and Y. Mei, "Shape memory alloy helical microrobots with transformable capability towards vascular occlusion treatment," *Research*, vol. 2022, pp. 1–13, Jan. 2022.
- [19] N. Shinjo and G. W. Swain, "Use of a shape memory alloy for the design of an oscillatory propulsion system," *IEEE J. Ocean. Eng.*, vol. 29, no. 3, pp. 750–755, Jul. 2004.
- [20] Z. Wang, G. Hang, J. Li, Y. Wang, and K. Xiao, "A micro-robot fish with embedded SMA wire actuated flexible biomimetic fin," *Sens. Actuators A, Phys.*, vol. 144, no. 2, pp. 354–360, Jun. 2008.
- [21] J.-S. Koh and K.-J. Cho, "Omegabot: Biomimetic inchworm robot using SMA coil actuator and smart composite microstructures (SCM)," in *Proc. IEEE Int. Conf. Robot. Biomimetics (ROBIO)*, Dec. 2009, pp. 1154–1159.
- [22] H.-T. Lin, G. G. Leisk, and B. Trimmer, "GoQBot: A caterpillar-inspired soft-bodied rolling robot," *Bioinspiration Biomimetics*, vol. 6, no. 2, Jun. 2011, Art. no. 026007.
- [23] P. Arena, C. Bonomo, L. Fortuna, M. Frasca, and S. Graziani, "Design and control of an IPMC wormlike robot," *IEEE Trans. Syst., Man Cybern. B, Cybern.*, vol. 36, no. 5, pp. 1044–1052, Oct. 2006.
- [24] B. Kim, J. Ryu, Y. Jeong, Y. Tak, B. Kim, and J.-O. Park, "A ciliary based 8-legged walking micro robot using cast IPMC actuators," in *Proc. IEEE Int. Conf. Robot. Autom.*, Sep. 2003, pp. 2940–2945.
- [25] S. Guo, T. Fukuda, and K. Asaka, "A new type of fish-like underwater microrobot," *IEEE/ASME Trans. Mechatronics*, vol. 8, no. 1, pp. 136–141, Mar. 2003.
- [26] Z. Chen, S. Shatarra, and X. Tan, "Modeling of biomimetic robotic fish propelled by an ionic polymer–metal composite caudal fin," *IEEE/ASME Trans. Mechatronics*, vol. 15, no. 3, pp. 448–459, Jun. 2010.
- [27] J. M. Morrey, B. Larribrecht, A. D. Horchler, R. E. Ritzmann, and R. D. Quinn, "Highly mobile and robust small quadruped robots," in *Proc. IEEE/RSJ Int. Conf. Intell. Robots Syst. (IROS)*, Oct. 2003, pp. 82–87.



**SHUAIBY MOHAMED** (Member, IEEE) received the M.Sc. degree in mechatronics engineering from Assiut University, Egypt, in 2013, and the Ph.D. degree in robotics from Toyohashi University of Technology, Japan, in 2017. Since 2018, he has been an Assistant Professor with Assiut University. He was a Postdoctoral Researcher with the HRI Laboratory, Kyoto University, in 2022. Currently, he is a Postdoctoral Researcher with Hanbat National University. His research interests include robotics, mechatronics, and electromagnetic actuator. He is a member of the Robotics and Automation Society.



**YOUNGWOO IM** received the M.Sc. degree from the Department of Mechanical Engineering, Hanbat National University, in 2024. His research interests include mechanical design, mechatronics, and mobile robots.



**HYEONSANG SHIN** received the M.Sc. degree from the Department of Mechanical Engineering, Hanbat National University, in 2024. His research interests include mechanical design, mechatronics, and mobile robots.



**YOUNGSHIK KIM** received the M.Sc. and Ph.D. degrees in mechanical engineering from the University of Utah, in 2003 and 2008, respectively. Since 2011, he has been with Hanbat National University, where he is currently a Professor in mechanical engineering. His research interests include smart actuator, motion control, bio-inspired robot, and sensor fusion.



**BUHYUN SHIN** received the B.S. and Ph.D. degrees from the School of Mechanical and Aerospace Engineering, Seoul National University, in 2001 and 2007, respectively. Since 2012, he has been with Hanbat National University, where he is currently a Professor in mechanical engineering. His research interests include electromagnetic actuator, smart actuator, and bio-inspired robot.

...